2010 43rd Annual IEEE/ACM International Symposium on Microarchitecture

LOFT: A High Performance Network-on-Chip Providing Quality-of-Service Support

Jin Ouyang* and Yuan Xie
Computer Science and Engineering Dept., the Pennsylvania State University
*jouyang@cse.psu.edu

Abstract

*Providing quality-of-service (QoS) for concurrent tasks in many-core architectures is becoming important, especially for real-time applications. QoS support for on-chip shared resources (such as shared cache, bus, and memory controllers) in chip-multiprocessors has been investigated in recent years. Unlike other shared resources, network-on-chip (NoC) does not typically have central arbitration of accesses to the shared resource. Instead, each router shares the responsibility of resource allocation. While such distributed nature benefits the scalable performance of NoC, it also dramatically complicates the problem of providing QoS support for individual flows. Existing approaches to address this problem suffer from various shortcomings such as low network utilization and weak QoS guarantees. In this work, we propose **LOFT** NoC architecture which features both high network utilization and strong QoS guarantees. LOFT is based on the combination of two mechanisms: **a) locally-synchronized frames (LSF)**, which is a distributed frame-based scheduling mechanism that provides flexible QoS guarantees to different flows and **b) flit-reservation (FRS)**, which is a flow-control mechanism integrated in LSF that improves network utilization. The experimental results show that LOFT delivers flexible and reliable QoS guarantees while sufficiently utilizes available network capacity to gain high overall throughput.*

1. Introduction

The diminishing return from *instruction level parallelism* (ILP) has led the semiconductor industry toward utilizing *task level parallelism* (TLP) with chip-multiprocessors (CMP) and multiprocessor system-on-chip (MPSoC). For both commercial products [1]–[3] and research prototypes [4], [5], the number of processors on a single chip is increasing. For future large scale CMPs and MPSoCs, delivering sufficient bandwidth for on-chip communication is both critical to performance and challenging. Among various on-chip interconnect candidates, network-on-chip (NoC) has excellent scalability in that the throughput it can provide is proportional to its complexity and energy consumption. Therefore it is envisioned to be a solution for interconnecting tens to hundreds cores for future many-core architectures.

This work is supported in part by NSF 0905365, 0903432, 0702617, 0643902 and SRC grants.

Besides good overall throughput, it is becoming increasingly important to provide QoS support in many-core architectures for individual tasks, especially for real-time tasks. QoS support helps real-time tasks to maintain the expected performance and functionalities. It also enables *composability* and simplifies system integration during design time. Finally, QoS support enables performance isolation, which benefits the effectiveness of system-level task scheduler. Consequently, we have seen significant recent research efforts on QoS support in on-chip shared resources such as caches [6]–[8] and memory controllers [9]–[11].

However, providing QoS guarantees with NoC turns out to be difficult, because tens and hundreds of tasks compete for bandwidth while the scheduling is distributed to each router. The lack of global knowledge hinders implementing robust QoS guarantees with straightforward schemes. To address this difficulty, existing approaches to provide QoS support rely on resource reservations or relaxing guarantees, resulting in either low network throughput or weak guarantees.

The focus of this work is to design a new NoC architecture that can provide strong and flexible QoS support, and at the same time can sufficiently utilize network bandwidth to achieve high overall performance. Our proposed *LOFT* network-on-chip architecture achieves the above goal based on the combination of two mechanisms:

- **Locally-Synchronized Frame** (LSF) is a frame-based scheduling mechanism implemented locally in each router, in order to provide strong and flexible service guarantees to respective flows. In LSF, the distributed scheduling within each router only requires local information exchange between adjacent routers, without the need of global knowledge. Therefore, LSF is well scalable, especially suitable for future large scale multiprocessor architectures.
- **Flit-Reservation** (FRS) is a flow-control mechanism bound to LSF and improves overall network utilization and throughput. In FRS, a *look-ahead flit* is sent before the *data flits*, to reserve bandwidth and buffers along the path to the destination. The data flits follow the look-ahead flit and reclaim resources booked by the look-ahead flit to make progress. Look-ahead flits are routed on a separate *look-ahead network* without interfering with data flits. Since look-ahead flits are much shorter than data flits, the *look-ahead* network is lightly loaded and quite fast.

The contribution of LOFT can be generalized as follows: *a)* LOFT can provide robust throughput guarantee to each rate-observing flow even with interference of malicious aggressors that try to exhaust network bandwidth; *b)* LOFT also guarantees delay bound at a much finer granularity than similar approaches [12], [13]; *c)* LOFT can fully exploit under-utilized bandwidth, and achieve excellent overall performance; *d)* the extra hardware introduced by LOFT is light-weight, incurring very low overheads.

2. Background

In this section, we first describe the required features in a network-on-chip architecture that can provide quality-of-service. We then review related work on quality-of-service (QoS) and guaranteed service (GS) support for network-on-chip (Guaranteed service support can be viewed as a special problem of QoS. However, some NoC literatures use the terms interchangeably, both referring to mechanisms that provide bandwidth or latency guarantee).

2.1. Quality-of-Service in Network-on-Chip

We assume a general model as follows. In a multi-hop NoC connected by routers, multiple processing elements (PE) send data to each other. A $flow$ refers to the unique traffic sent from one PE (source) to another PE (destination). Flows are uni-directional. We use $flow_{ij}$ to refer to the traffic from node i to node j and *vice versa*. A single node can be sources as well as destinations of multiple flows. Some links in NoC are used by several flows, which effectively share the link bandwidth. For a certain flow requiring quality-of-service, say $flow_{ij}$, it exposes its requirements as minimum throughput r_{ij} and maximum delay bound b_{ij}. With this model, the desired features of QoS support in NoC is specified as follows:

(a) Guaranteed minimum throughput: For $flow_{ij}$ requiring quality-of-service, its data rate is at least r_{ij} regardless of other flows contending for bandwidth.

(b) Guaranteed maximum delay: During design phase, it should be possible to calculate the maximum packet delay b_{ij} according to the path taken by $flow_{ij}$. This can be used by various design-time procedures such as task binding and route computation. During run-time, the actual maximum packet delay should be always less than the previously calculated bound.

(c) Fairness in throughput allocation: It should allow contending flows to specify either equal or differentiated data rates (**fair allocation** or **differentiated allocation**). During run-time the actual data rates obtained are proportional to the specified data rates. As a *priori*, requirements **(a)** and **(b)** should be satisfied.

(d) Low level of under-utilization: It is not likely that a flow will be constantly using its booked throughput. Also, the full capacity of the network might not be totally booked. In either case, other flows should be able to scavenge the excess bandwidth to help performance.

(e) Low hardware complexity: The QoS mechanism is desirable to introduce little hardware overheads.

2.2. Related Work

A number of previous studies have developed mechanisms to provide quality-of-service and guaranteed service in NoC. Time-division-multiplexing (TDM) circuit-switching is proposed to provide bandwidth and latency guarantees in Æthereal NoC [14]. Each guaranteed flow is mapped to a virtual circuit, by reserving a time slot for each link along the path. By time-slot reservation, Æthereal architecture can provide the exact bandwidth booked by the flow and analyzable delay bounds. However, it does not allow guaranteed flows to use excess bandwidth when the network is under-utilized. Also, how to arbitrate amongst throughput requests is not clear from the original work. Nostrum NoC [15] also exploits the idea of TDM to create virtual circuits and uses the so-called "containers" to provide bandwidth guarantee. It only works for deflective routing and shares the same problem with Æthereal. In MANGO NoC [16], a flow needs to reserve the virtual channels along its path to construct a virtual circuit before sending packets on the virtual circuit. Therefore MANGO implements a large amount of buffers and complex switch modules. In addition, this connection-based approach tends to penalize short-lived transactions and compromises the overall throughput. In SonicsMX [17], sources insert interval markers to acquire bandwidth. The benefit of this approach is the absence of circuit setup. However, it does not provide hard guarantees of either minimum bandwidth or maximum delay.

Our work is closely related to Globally-Synchronized Frames (GSF) [12] and its extension [13]. GSF adopts the frame-based scheduling principles proposed in Rotate Combined Queues (RCQ) [18] and offers excellent throughput guarantees. In GSF, time is coarsely quantized into frames, and each flow can reserve a fraction in the frame to inject data flits. Frames are prioritized according to their ages, and the data flits belonging to older frames are switched first in any router. GSF also allows bursty flows to utilize excess bandwidth by providing multiple on-the-fly frames and fast frame recycling. Without circuit setup and dedicated virtual channels, GSF has relatively low hardware complexity and good scalability.

However, GSF suffers from several problems. First, as suggested by Grot et al [13] and Das et al [19], to maintain a good performance GSF needs large frame sizes and source queues. For example, to achieve good throughput in a 64-node NoC, GSF needs a 2000-flit source queue [13], [19] which translates to a significant buffer overhead. In addition, the use of a large frame size causes the delay bounds to be too loose.

Second, the globally synchronized frame recylcing in GSF limits its ability to utilize excess bandwidth. Figure 1 shows an example pathological scenario. The grey nodes on the first column of the network are sending packets to the black node (hotspot) at the center of the network. The stripped node, in contrast, is sending to its nearest neighbor. Without prior knowledge of the actual traffic pattern (which is typically the case for CMP), all the nodes may be assigned equal reservations in the frame. In the actual traffic pattern, the stripped node could exploit full link speed since it experiences

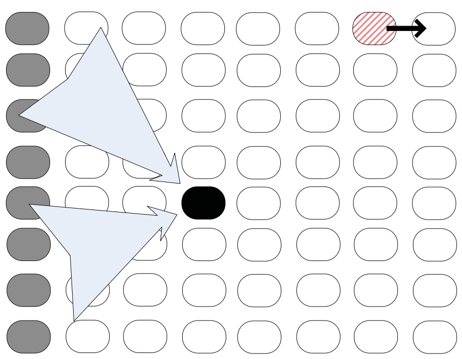

Fig. 1. A pathological scenario: while the stripped is not contending with the grey nodes, its throughput is still reduced by GSF due to the global synchronization

no contention. However, the pressure created on the hotspot node slows down the global frame recycling, which indirectly reduces the accepted throughput of the stripped node.

Third, GSF reduces the efficiency of virtual channel flow-control. To prevent priority inversion, GSF does not allow flits belonging to different packets to reside in the same virtual channel. This requirement essentially elongates the time to return virtual credits and further compromises the network throughput.

Our work is also related to the original work on flit-reservation by Peh *et al.* [20]. In Peh's work, flit-reservation is used entirely to improve the average performance, while in our work it is integrated into frame-based scheduling to offer guaranteed service.

3. Principles of LSF and FRS

Our proposed LOFT architecture is based on the integration of locally-synchronized frames (LSF) and flit-reservation flow-control (FRS). In this section, we separately present the principles for LSF and FRS, but defer the discussion of integration of LSF and FRS to the next section.

3.1. Frame-Based Scheduling

Both GSF [12] and *locally-synchronized frames* (LSF) are based on the idea of grouping time slots into frames, to coarsely approximate the ideal deadline-based scheduling [21]. The term "scheduling" in the NoC sense is to determine the switching order of flits contending for an output physical link. Figure 2a showcases how contentions in the NoC can be abstracted by a server model. As can be seen, "server" here simply refers to each physical link, and the "service" it provides is the link bandwidth. At each server, queues (buffers) are provided to account for dynamic mismatch between arrival and service rates. Scheduling is performed conceptually by a "MUX", which at each cycle dequeue one flit from a certain queue to service. Therefore the dequeuing order determines the service order.

Using this model, frame-based scheduling can be explained with the help of Figure 2b and 2c. First, Figure 2b shows

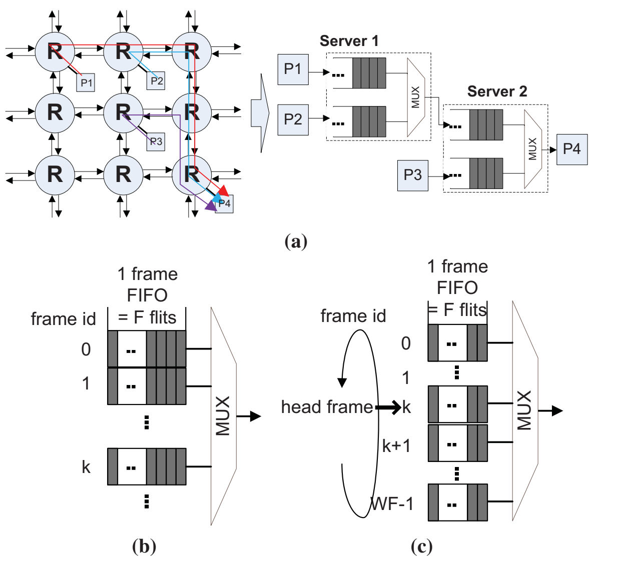

Fig. 2. (a) Abstraction of network contention into a server model. The left part shows a piece of NoC; and the right part shows the converted server model. The rectangles labeled "P" represent PEs; the circles labeled "R" represent routers. In this figure three contending flows are shown. Flows are merged at each scheduling point, where a "MUX" picks flits from different queues in a certain order. For simplicity, PEs other than sources or destinations and routers without contention are omitted. (b) and (c) Frame-based arbitration: (b) shows the ideal setup while (c) shows the practical setup

the ideal setup. At each "MUX" (the scheduling point), the buffers are divided into isolated queues, the *frames*. Each frame has a size of F flits. Frames are associated with a frame number, and the smaller this number is, the higher priority the corresponding frame has. The "MUX" services the flits in the frames in the decreasing order of their priorities. That is, "MUX" will first dequeue flits from frame 0, and only after all flits in frame k are drained, the flits in frame $(k+1)$ can be serviced. A *head frame* pointer points to the frame currently being serviced, the *head frame*. Figure 2c shows a more practical setting, where there is a finite window of frames, which has WF frames. The head frame pointer walks across frames in the round-robin order.

Incoming flits are queued into frames as follows. For each contending $flow_{ij}$ at "MUX", it is assigned a fixed number of buffer slots, denoted by its allocated reservation R_{ij}, from each frame. The sum of R_{ij}s cannot be larger than F. $flow_{ij}$ can only inject up to R_{ij} flits of its incoming flits into a frame, starting from the highest priority frame. The flow is throttled if its injection frame hits the head frame; that is, its reservations in all the frames have been used up. A throttled flow can restart to inject flits when the head frame pointer advances, at which time the frame window is shifted by 1. Frame window shifting effectively recycles the oldest frame to a fresh one.

Allocating buffer slots inside each frame essentially divides the total bandwidth into shares. If we assume that the "MUX" can dequeue 1 flit at a cycle, and $\sum R_{ij} \leq F$, then the throughput allocated to $flow_{ij}$ is $R_{ij}/\sum R_{ij}$ of the ideal bandwidth. In addition, since at most only F flits can be injected into a frame, the time to drain the head frame is upper bounded.

While based on the same principle, GSF and LSF fundamentally differs in where frames are managed. GSF abstracts the whole NoC as a single "MUX". In GSF, frame window shifting is globally synchronized by a barrier network. While this saves some complexities in the router, it also incurs serious problems as discussed in Section 2.2. In contrast, in LSF each output link of a router manages frame recycling of its own frames regardless of other output links or routers. The benefit of doing so will become clear from the following sections. In addition, LSF allows for integration of flit-reservation, an efficient flow-control mechanism to improve performance.

3.2. Flit-Reservation

Flit-reservation flow-control (FRS), originally proposed by Peh et al [20], is an integral part of LOFT. It meshes with LSF well since it is also a distributed resource scheduling mechanism. As [20] presented a thorough discussion, here we only briefly reiterate the key ideas.

FRS proposes using *look-ahead flits* to pre-schedule bandwidth and buffers for *data flits*, and thus obliterates the need of arbitration and flow-control for data flits. A *look-ahead network* is dedicated to route look-ahead flits. The look-ahead network is simply a second physical network overlaid on the data network. Before the injection of any data flit, a leading look-ahead flit must be injected into the look-ahead network to reserve resources for the data flit.

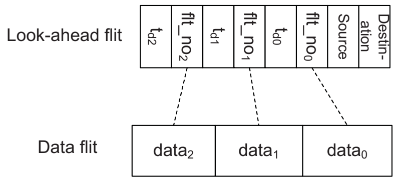

Fig. 3. Format of look-ahead flits.

Figure 3 shows the format of look-ahead flits. The look-ahead flit contains the departure times (t_d) and the flit numbers (flt_no) for the data flits it leads. A look-ahead flit can leads only data flits belonging to a single flow. A source field uniquely identifies the source node of the flow, and a destination field identifies the destination node. Each flt_no field uniquely identifies a data flit led by the look-ahead flit, and each t_d following the flt_no records the departure time of that data flit from the previous router. While originally in [20] flt_no and the source field are not needed, for integration with LSF we introduce these two fields, whose usage will be clear in Section 4.

The router architectures for both the look-ahead network and the data network are shown in Figure 4. The router of the look-ahead network closely resembles the generic wormhole router with virtual channels and a sequence of routing stages: route computing (RC), virtual channel allocation (VA), switch

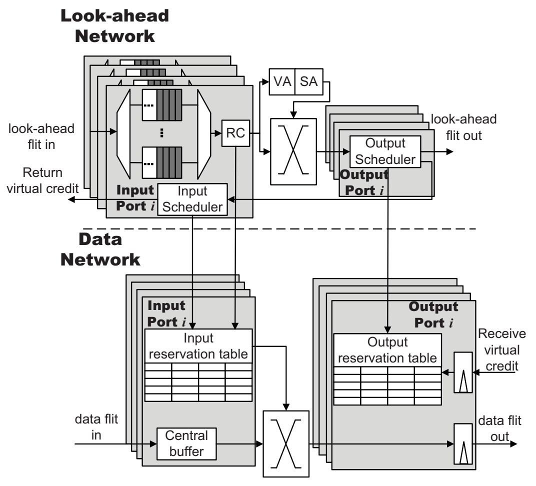

Fig. 4. Router architecture for flit-reservation flow-control.

Time Slot	0	1	2	3	4	5	6	7
Busy Flag						X		
Virtual Credits	1	3	1	0	0	0	1	2

(a) **Output reservation table**

Time Slot	0	1	2	3	4	5	6	7
Flow No.			M					
Flit No.			N					
Input Buffer			3					
Switch Time			+2					
Buffer Out					3			
Output Port					E			

(b) **Input reservation table**

Fig. 5. The formats of reservation tables.

allocation (SA), and switch traversal. In addition, each output/input port of the router contains an output/input scheduler. The output scheduler schedules the departure times of data flits to the next router. The input scheduler allocates space in the input buffer for data flits, and schedules data flits to traverse the switch to output ports in time before departure. Both schedulers program the scheduled events in the output and input reservation tables respectively.

The data network router contains an output reservation table in each output port, and an input reservation table in each input port. These tables contain the scheduling results from the schedulers to manipulate the movement of data flits. In addition, the input buffer is arranged as a central buffer, rather than virtual channels.

The formats of output reservation table and input reservation tables are shown in Figure 5. The output reservation table keeps track of the status of the output port within a time window, which in this figure has 8 time slots. For each time slot, it contains a busy flag to record if the output port is busy. It also contains a field to record the number of free buffer slots

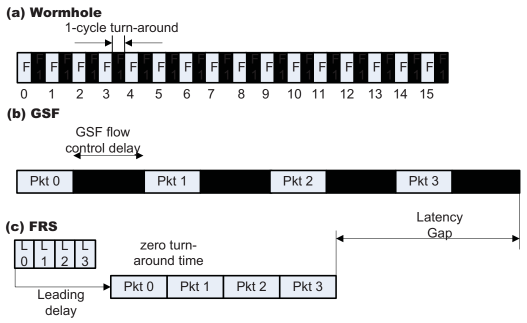

Fig. 6. Comparison of three different flow-control mechanisms. The black rectangles reflect credit turn-around time. For wormhole, the rectangles labeled "F" represent flits. For VCT and FRS, the rectangles labeled "Pkt k" represent packets. The rectangles labeled "L k" in FRS refer to look-head flits.

in the input buffer of the next router. We refer to this field "virtual credits" as it represents free buffers in future time slots rather than the current time slot. The grey arrow in the figure indicates the current time slot. The input reservation table is organized similarly, recording the information of arriving data flits (flow and flit number). In addition, it stores buffer allocation, output ports, and switching times of arriving data flits.

The procedure of scheduling the departure time of a data flit is sketched as follows:
1) The look-ahead flit arrives at a router, and writes the information of data flits it leads to the input reservation table. Buffers are also allocated for the data flits.
2) The look-ahead flit passes the router pipeline as in an ordinary router.
3) When the look-ahead flit reaches the output port, it tries to schedule the earliest departure times (when the output port is not busy and the virtual credit count is positive). Upon successful scheduling, it updates the status of the output reservation table.
4) The output scheduling result is returned to the input scheduler, which updates the switching time and the output port. The input scheduler also returns virtual credits to the previous router.
5) When data flits arrive, the input scheduler *lazily* allocates buffer slots for them.

For example, Figure 5 shows the status of reservation tables after scheduling one data flit which arrives at cycle 2 and is scheduled to departure at cycle 5 from the east port.

Figure 6 presents a comparison of flow-control mechanisms in conventional wormhole switching, GSF, and FRS, which highlights the efficiency of FRS. This time graph shows the back-to-back transfer of 4 packets each having 4 flits between two routers when the input buffer is close to full. As can be seen, even assuming 1-cycle credit turn-around time, flow-control introduces a non-negligible throughput overhead to wormhole switching. This overhead is even worse for GSF. On the other hand, FRS can achieve zero turn-around time and has the highest efficiency. In addition, as the look-ahead flits are short and a single look-ahead flit can schedule multiple data flits, the look-ahead network is lightly loaded and fast.

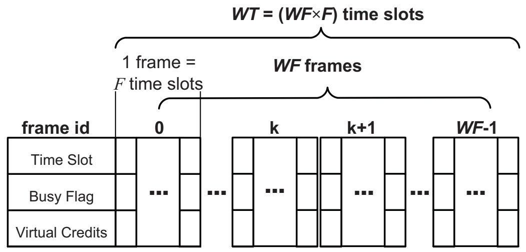

Fig. 7. Integration of LSF and FRS: the time slots in output reservation tables are grouped into frames.

4. Integration of LSF and FRS

Locally-synchronized frames and flit-reservation share fundamental similarities. Both mechanisms are forms of distributed resource scheduler that allocates buffer space and link bandwidth. In addition, the central buffer used by FRS can be readily used to emulate the frame queues used by LSF. The similarities motivate us to combine the two mechanisms for a high performance network-on-chip providing guaranteed services. We discuss the integration of LSF and FRS in this section.

4.1. Combining Local Frames and Reservation Tables

The first step we take is to divide the output reservation table, rather than input buffers, into frames (Figure 7). The frame size F now equals to the number of time slots in each segment of the framed output table. A share of time slots, denoted as R_{ij}, from each frame is assigned to each $flow_{ij}$ contending for the output. Using the same terminology as frame-based scheduling, successfully scheduling a time slot in a frame k is referred to as injecting a data flit into frame k. As with frame-based scheduling, each $flow_{ij}$ can only inject up to R_{ij} data flits into each frame, and it is required that $\sum R_{ij} \leq F$.

Each output scheduler maintains a current time slot pointer (denoted as CP) indicating the current time slot, and a head frame pointer (denoted as HF) pointing to the frame being serviced. Each $flow_{ij}$ contending for the output link maintains its current injection frame IF_{ij} and remaining reservation C_{ij}. WF is used to denote the frame window size and WT is used to denote the time window size, where $WT = F \times WF$.

Algorithm 1 formally shows the injection procedure for $flow_{ij}$. When the network is powered-up, IF_{ij} is initialized to HF and C_{ij} is initialized to R_{ij}. Upon each scheduling request from look-ahead flits belonging to $flow_{ij}$, it is first checked if C_{ij} is positive. If so, procedure $try\_schedule()$ is invoked to try to inject the data flit into frame IF_{ij}. Upon successful scheduling, C_{ij} is decremented by one; otherwise, IF_{ij} is incremented and C_{ij} is updated to the minimum of

Algorithm 1 Injection procedure for $flow_{ij}$

```
Initialize: $IF_{ij} \leftarrow HF$
Initialize: $C_{ij} \leftarrow R_{ij}$
UPON EVERY REQUEST FROM LOOK-AHEAD FLITS:
$scheduled \leftarrow FALSE$
while $scheduled = FALSE$ do
    if $C_{ij} > 0$ then
        $scheduled \leftarrow try\_schedule(IF_{ij})$
    end if
    if $scheduled$ then
        $C_{ij} \leftarrow C_{ij} - 1$
    else
        if $(IF_{ij} + 1) \text{Mod}\, WF \neq HF$ then
            $C_{ij} \leftarrow MIN(R_{ij}, C_{ij} + R_{ij})$
            $IF_{ij} \leftarrow (IF_{ij} + 1) \text{Mod}\, WF$
        else
            break
        end if
    end if
end while
```

Algorithm 2 $try\_schedule(IF_{ij})$

```
if $IF_{ij} = HF$ then
    $candidate \leftarrow CP + 1$
else
    $candidate \leftarrow F \times IF_{ij}$
end if
$scheduled \leftarrow FALSE$
while $scheduled = FALSE$ and $candidate \neq ((IF_{ij} + 1) \text{ Mod } WF) \times F$ do
    if output_table($candidate$).busy $= FALSE$ and output_table($candidate$).virtual_credit $> 0$ then
        $schedule \leftarrow TRUE$    // Scheduling is successful if a valid slot is found
    else
        $candidate \leftarrow candiate + 1$
    end if
end while
if scheduled then
    Update output and input reservation tables
end if
return $scheduled$
```

R_{ij} and $(C_{ij} + R_{ij})$, until the reservations in all frames have been exhausted.

Algorithm 2 defines procedure $try\_schedule()$. In the algorithm, we use output_table(k).busy and output_table(k).virtual_credits to refer to the busy flag and the virtual credit count of entry k in the output reservation table. We define a valid time slot as the slot with a false busy flag and a positive virtual credit count. Procedure $try\_schedule()$ only returns true if a valid time slot is found in the given injection frame.

Algorithm 3 shows the procedure to shift the frame window. Initially CP and HF are both assigned “0”. At each cycle CP is updated to $(CP + 1) \text{Mod}\, WT$, while HF is updated to $(HF + 1) \text{Mod}\, WF$ for every F cycles.

It is worth to mention that GSF [12] does not allow flows to inject into the head frame, in order to guarantee that the head frame is drained in a finite time. In contrast, in our work injection to head frame is permitted, as it is guaranteed that the head frame can be recycled for every F cycles.

Algorithm 3 Manipulation of CP and HF

```
Initialize: $CP \leftarrow 0$ $HF \leftarrow 0$
AT EVERY CLOCK TICK:
$CP \leftarrow (CP + 1) \text{Mod}\, WT$
if $CP \text{ Mod } F = 0$ then
    for all $flow_{ij}$ contending for the output link do
        if $IF_{ij} = HF$ then
            $IF_{ij} \leftarrow (IF_{ij} + 1) \text{Mod}\, WF$
            $C_{ij} \leftarrow MIN(R_{ij}, C_{ij} + R_{ij})$
        end if
    end for
    $HF \leftarrow (HF + 1) \text{Mod}\, WF$
end if
```

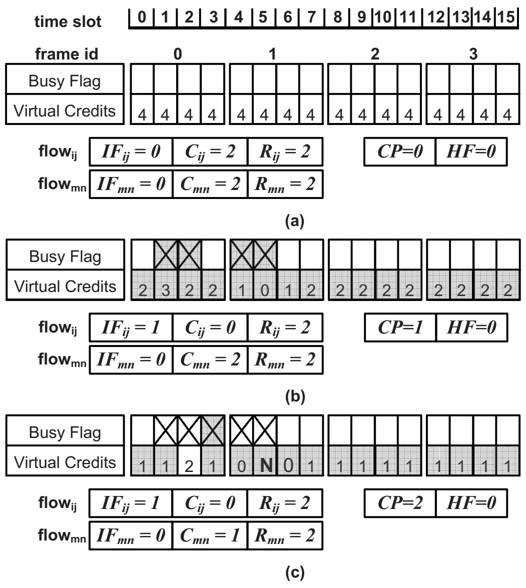

Fig. 8. An example showing *output scheduling anomaly*. The entry tagged by “**N**” shown in (c) indicates buffer underflow.

4.2. Output Scheduling Anomaly

While the construction in the previous subsection seems plausible, it has an inherent severe problem, which is explained by the following example.

Consider a simplified case where two flows $flow_{ij}$ and $flow_{mn}$ contend for an output link. Suppose $F = 4$, $WF = 4$, and the size of input buffer is 4 flits. We equally distribute the link bandwidth to the two flows; that is, $R_{ij} = R_{mn} = 2$. The initial status of the output reservation table is shown in Figure 8a.

Now suppose two look-ahead flits from $flow_{ij}$ arrive in the first two cycles, and each of them leads two data flits. The first look-ahead flit will successfully schedule two time slots in the first frame. Then the second look-ahead flit finds its reservation in frame 0 is used up. Therefore it advances IF_{ij} and injects two data flits in the second frame. Furthermore, the virtual credits consumed in the first frame are not returned by slot 7 (this is possible, for example, due to contention in the next hop). The output reservation table immediately after the previous scheduling events is shown in Figure 8b (shaded entries indicate changes). It shows that the next input buffer is full at slot 5 with zero virtual credits. A problem may occur if a look-ahead flit from $flow_{mn}$ arrives in the third cycle, leading one data flit. This look-ahead flit will inject to frame 0, since it has $C_{mn} > 0$ and finds slot 3 is valid. However, the virtual credit count at slot 5 will become negative after $flow_{mn}$ injects to slot 3 (Figure 8c)! The outcome is disastrous since the buffer is "silently" overbooked without any flow being aware. At cycle 5, the actual delivery of the scheduled data flit may fail due to insufficient buffer.

We call this problem *output scheduling anomaly*, which is a direct consequence of out-of-order scheduling as shown in the above example. An aggressive flow can schedule buffer slots in more distant future, as forced by frame-based scheduling. A more moderate flow not aware of the aggressive flow may inject to a more imminent time slot, which may cause buffer underflow in the future. There are two straightforward approaches to address the problem. The first approach prevents injection into a time slot if any future time slot has zero credits. The second approach enforces in-order scheduling by requiring new data flits to be scheduled in more distant time slots than any already scheduled data flits. While either approach eliminates the anomaly, both of them will force a moderate flow to discard unused reservations in more imminent frames. This would cause bandwidth under-utilization and break the fairness of scheduling. A better solution to the anomaly problem should let aggressive flows voluntarily yield buffer space to moderate flows.

Our solution to the problem introduces an additional counter $skipped(i)$ associated with each frame i, where $i \in [0, WF-1]$. Informally, $skipped(i)$ records the total yielded reservations by all flows. The manipulation of $skipped(i)$ is as follows:

1) Upon initialization, $skipped(i) \leftarrow 0$.
2) When the injection pointer IF_{ij} of a $flow_{ij}$ advances, $skipped(IF_{ij})$ is incremented by C_{ij}. That is, we add $skipped(IF_{ij}) \leftarrow skipped(IF_{ij}) + C_{ij}$ after the **if** statement in line 12 of Algorithm 1.

The newly added counter $skipped(i)$ is used as follows. For an arbitrary flow $flow_{ij}$, let $Prior$ be the index of the entry immediately prior to the injection frame IF_{ij} in the output reservation table. That is, $Prior$ equals to $(IF_{ij} \times F + WT - 1) Mod WT$. Then $flow_{ij}$ can only inject flits into frame IF_{ij} if the following condition holds:

$$F - skipped(IF_{ij}) \leq \text{out\_table}(Prior).\text{virtual\_credit} \quad (1)$$

Condition (1) is appended to the conditions of the **if** statement at line 6 of Algorithm 1. With this change, output scheduling anomaly is eliminated when the size of input buffer is F flits, as stated by Theorem I in the Appendix. In addition, aggressive flows will voluntarily yield buffer space to moderate flows to ensure fair allocation in buffer space. *Detailed discussion of condition (1) can be found in the Appendix.*

Reconsider our example with the addition of condition (1). Now $flow_{ij}$ cannot inject into frame 1 since $F - skipped(1) = 4 >$ out_table(3).virtual_credit $= 2$. Therefore it will advance IF_{ij} to 2, and as a result $skipped(1) = C_{ij} = 2$. Since now $F - skipped(2) = 4 \leq$ out_table(7).virtual_credit $= 4$, $flow_{ij}$ can inject two data flits into frame 2. After that, when $flow_{mn}$ schedules slot 3, no buffer underflow will occur.

4.3. Optimizations

The techniques presented so far frame output reservation tables to provide fair bandwidth allocation. However, although each output scheduler independently manages output reservation tables and frames, frame recycling is still globally synchronized across all routers using Algorithm 3. Consider the stripped node in Figure 1. Despite the ample bandwidth it could leverage, on average it can only inject R_{ij} flits for every F cycles and the bandwidth is under-utilized. In this subsection, we propose optimizations to improve utilization and overall throughput. The first optimization speculatively forwards flits to reduce latency. The second optimization breaks the global synchronization among schedulers to exploit excess bandwidth.

4.3.1. Speculative Flit Switching. In the present switching mechanism, data flits are switched at the time slot scheduled by look-ahead flits, even when no other flits are scheduled before them. This unnecessarily prolongs the delivery latency when the network is lightly loaded.

To address this problem, we modify the switching mechanism to forward data flits as soon as possible. A data flit can be forwarded to the next router if there is no on-going transmission on the output link and if the next buffer has free space. This requires two changes to the data network router shown in Figure 4. First, additional signals are added to return actual credits in the input buffer. Second, an output arbiter similar to the switch arbiter is needed to pick one flit from the ready data flits to forward. This arbiter can be a simple round-robin arbiter, since its choice will not compromise scheduling made by LSF and FRS, except for one case explained below.

The input scheduler picks a data flit that has arrived (input buffer has been allocated) with earliest scheduled departure time as the candidate for switching. In practice, it just picks the first non-empty entry in the "buffer out" row of the input reservation table. If the candidate wins the output arbitration, it will be forwarded and its entry in the input and output reservation tables will be cleared. The input scheduler will mark a candidate as *emergent* if it is scheduled to be forwarded in the current cycle. Emergent candidate is guaranteed to win arbitration. This causes no problem since an output port can only have at most one emergent candidate for each cycle. This is the only exception for the round-robin arbiter.

Two caveats deserves explanation. First, as now the data flits may arrive ahead of the scheduled time (but still after the look-ahead flit), the input reservation table needs to record the flow number and flit number, in order to uniquely identify arriving data flits. This information is provided by the look-ahead flit.

The second problem is more subtle but severe. With the modified switching mechanism, data flits may be serviced in a different order other than the scheduled order. This brings back the problem of *output scheduling anomaly*, where out-of-order forwarding may cause buffer underflow at a later time. The outcome is the potential risk that emergent flits miss their switching times due to insufficient buffer. We solve this problem by adding a “speculative buffer” to each input port, as shown in Figure 9. The speculative buffer is used to hold data flits forwarded out of order, and the original non-speculative buffer is used for in-order flits. The output reservation table only tracks buffer usage of the non-speculative buffer. For a winning candidate, the output scheduler checks if it is the first scheduled flit in the output reservation table. If so, the data flit is forwarded to the non-speculative buffer; if not, it is forwarded to the speculative buffer. In either case, if the corresponding buffer is full the data flit will be denied access to the output link. At the other end of the link, the input scheduler allocates space in the speculative buffer for speculative flits and *vice versa*. Using a separate speculative buffer prevents out-of-order flits from blocking emergent flits.

4.3.2. Local Status Reset. Speculative forwarding only saves latency but not improves throughput. A flow cannot inject more data flits once its reservation in a frame window is used up, even if all scheduled data flits have been delivered by speculative switching. The intrinsic bottleneck to throughput is the constant frame recycling rate for both lightly loaded and heavily loaded links. Thus we propose to do *local status reset* when an output link is idle. During a *local status reset* event, *a)* $CP, HF \leftarrow 0$, *b)* $IF_{ij} \leftarrow HF$, $C_{ij} \leftarrow R_{ij}$, for all contending $flow_{ij}$, and *c)* out_table(i).virtual_credit $\leftarrow B_N, \forall i \in [0, WT-1]$, where B_N is the size of the non-speculative buffer. The reset event is triggered on an output link when the conditions below are both met to ensure the reset is safe:

• All the busy flags in the output reservation table are $FALSE$.

• The non-speculative buffer in the next input port is empty. This can be checked by the credits returned from the non-speculative buffer.

Local status reset essentially recycles all the frames in the frame window to be fresh frames. It reduces the idle time of output link and improves utilization. Note that *local status reset* also breaks the global synchronization of frame recycling, allowing lightly loaded links to recycle frames at faster rates.

5. Simulation Setup

5.1. LOFT

We model LOFT adhering to the principles presented in Section 4 in a cycle-accurate NoC simulator [22]. Our current model simulates a 8×8 mesh topology. Each node is numbered by $(x + y \times 8)$ according to its coordinates (x, y). The injection rates of the source nodes are variable for the purpose of performance study. In contrast, the ejection rate of any destination is constant, 1 flit/cycle.

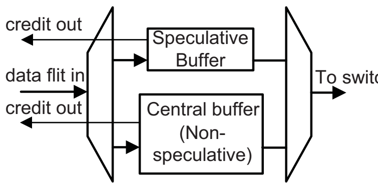

Fig. 9. The speculative and the non-speculative buffer sharing an input link.

TABLE 1. Simulation Setup

Common Specification			
Size & topology	64-node 2D mesh		
Routing algorithm	Dimension-order		
Maximum flows	64		
Packet size	4 flits		
LOFT			
Frame size	256		
Frame window size	2		
Time window size	128		
Look-ahead network		Data network	
No. of virtual channels	3	Depth of central buffer	256
Buffer size of each channel	4	Depth of spec. buffer	0–16 flits
No. of router stages	3	No. of router stages	3
Look-ahead flit width	64-bit	Data flit width	128-bit
		Reservation table size	256
GSF			
No. of virtual channels	6		
Buffer size of each channel	5		
Frame size	2000 flits		
Frame window size	6		
Barrier network delay	16 cycles		

The detailed specifications are generalized in Table 1. Each data packet has 4 data flits, which are further partitioned to two 2-flit *data quantum*. Each look-ahead flit leads a single data quantum, which is scheduled in its entirety to simplify scheduling. With $F = 256$ and $WF = 2$, this implies a reservation table size of $F \times WF/2 = 256$ entries. In addition, we assume that the maximum number of flows contending for a link is 64. With deterministic routing, we further assume that a flow uses the same reservation (R_{ij}) for all links of its path, and that for all contending $flow_{ij}$ of a link, $\sum R_{ij} \leq F$.

5.1.1. Look-ahead Network. The router architecture of look-ahead network adheres to that shown in Figure 4. We add one output scheduling stage (input scheduling is not on the critical path) to a baseline 2-stage wormhole router with look-ahead routing and speculative switch allocation [23]. Each output scheduler maintains the status (injection frame IF_{ij}, allocated reservation R_{ij}, and remaining reservation C_{ij}) for 64 flows as well as the head frame pointer HF and current slot pointer CP shared by all flows.

In the current setup, each look-ahead flit leads a single data quantum composed by 2 data flits. Therefore the flit number (departure time) simply becomes the *quantum* number (departure time). The 32-bit look-ahead flit contains a 6-bit destination field, a 6-bit flow number field, a 10-bit quantum number field, and a 10-bit departure time field.

5.1.2. Data Network. The router in the data network also has 3 stages: input buffer allocation, output request and arbitration, and switch traversal. The depth of the central buffer (non-speculative) is set to the same as the frame size to eliminate output scheduling anomaly (see Section 4.2). The depth of the speculative buffer is varied from 0 to 16 flits, and the impact of its size is studied.

Each data flit is 128-bit wide, same as the link width. The unique flow number and flit number is stored in the first 16 bits. Note that data flits do not contain any routing and scheduling information, as routing and scheduling has been done by the leading look-ahead flits.

5.2. GSF

For comparison purpose, we also implement GSF in the simulator. The suggested parameters in [13] and [19] are used, which are shown in Table 1. The network size, topology, injection and ejection rates, and routing algorithm are the same as LOFT. To maintain an acceptable performance, GSF requires a source queue as large as the frame size (2000 flits) for each node.

5.3. Delay Bounds and Hardware Cost

From the specifications in Table 1, we can calculate delay bounds and hardware cost of both LOFT and GSF.

5.3.1. Delay Bounds. As explained by [12], injected packets in GSF are guaranteed to be drained in one frame window. However, a tight bound of the period of the frame window is difficult to estimate, and the original work [12] relies on simulation to obtain an empirical bound. Nevertheless, a worst-case estimation can be made by assuming a frame window full of flits are injected to node 0 and destined to node 63. Then the worst-case time to drain a frame window is over $(k \times WF \times F)$. The factor k is due to the flow-control overhead (Section 3.2) and equals to 2 with the router architecture we model. Therefore the worst-case latency amounts to 24000 cycles. This bound is not only too long but regardless of paths taken by data flits. In contrast, LOFT provides much tighter bounds. In the worst case, all links in the network are heavily loaded, such that speculative switching and local status reset are not effective. In this case the worst-case end-to-end latency of LOFT is the same as that of RCQ [18]:

$$F \times WF \times Num\_Hops \qquad (2)$$

which amounts to 512 cycles per hop in our setting. Compared to GSF, this worst-case latency is not only much tighter but related to the paths taken by the flows.

5.3.2. Hardware Cost. As shown by Table 2, LOFT uses 32% less storages than GSF (assuming a 12-flit speculative buffer for LOFT). In addition, for a rough estimation of area and power, we use McPAT [24] with configurations to emulate the LOFT router (*e.g.*, a worm-hole NoC router with one virtual channel and 256-flit input buffer depth). The area and the power of a 64-node LOFT NoC are estimated to be 32mm^2 and 50W, which is 7% of a 64-node CMP [25] and 19% of total chip power (265W estimated by McPAT).

TABLE 2. Per Router Storage Requirements (bits)

GSF				
Source queue		Virtual channels		**Total**
256000		15360		271379
LOFT				
Input buf.	Reserv. tables	Flow stat.	Look-ahead network	**Total**
139264	40960	2308	1536	184203

6. Experiment Results

We measure and compare the quality-of-service metrics of LOFT and GSF, using the simulation setup presented in the previous section. In the simulation we run 4 types of synthetic traffic patterns: *uniform*, *hotspot*, and two pathological cases that evaluate the quality of performance isolation. For *uniform* traffic, each source is treated as a separate flow, while in other cases each source-destination pair is treated as a distinct flow. For *hotspot* traffic, all sources send packets to node 63. The configurations of the two pathological cases will be discussed later with their results. We run each simulation until a stable network state is reached. For clarity, in this section we use $flow_{i \to j}$ to refer to $flow_{ij}$.

6.1. Fairness

We first evaluate the general fairness of LOFT. Figure 10a, 10b and 10c show the results for equal and differentiated allocations respectively for *hotspot* traffic. For equal allocation, the bandwidth is distributed equally to all flows; in the two differentiated allocation cases, the network is divided into 4 and 2 partitions, and differentiated services are provided to different partitions. It can be seen that LOFT achieves excellent fairness in bandwidth allocation as GSF [12]. We repeat the same experiment for *uniform* pattern and confirm that the actual bandwidths received by different flows also comply with the allocation.

6.2. Performance

For performance evaluation, two metrics are used: *a)* average packet latency against offered load rate, and *b)* network throughput. We obtain the metrics from the simulation of *uniform* and *hotspot* traffics. For LOFT, we also vary the size of the speculative buffer to study its impact on performance. Note that setting the speculative buffer size to 0 is equivalent to turning off all optimizations proposed in Section 4.3. For comparison purpose, the performance of GSF is also measured and included in the results.

Figure 11a shows the result for *uniform* traffic pattern. The first observation from the result is that the average packet latency levels out when the offered load increases beyond a certain point for both LOFT and GSF. This is an expected result as to provide guaranteed service, both LOFT and GSF regulate the injection rates of flows and prevent unbounded packet latency. Second, we observe that increasing the speculative buffer size helps improve LOFT's performance, and LOFT outperforms GSF when the speculative buffer size is at least 8. However, increasing the speculative buffer size beyond 12 flits sees only marginal gains.

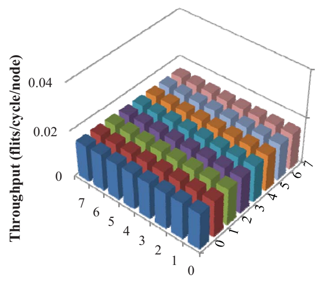

MAX	MIN	AVG	STDEV
0.157	0.154	0.156	0.4%

(a) Fair allocation

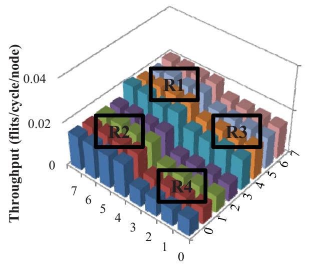

	MAX	MIN	AVG	STDEV
R1	0.0207	0.0188	0.0199	2.7%
R2	0.0156	0.1510	0.154	1.2%
R3	0.0154	0.0142	0.0147	2.3%
R4	0.0079	0.0078	0.0078	0.2%

(b) Differentiated allocation #1

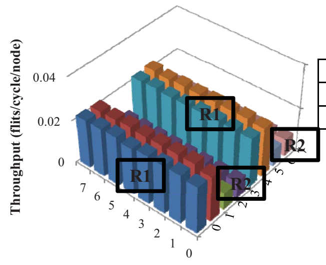

	MAX	MIN	AVG	STDEV
R1	0.0235	0.0209	0.0226	2.5%
R2	0.0079	0.0077	0.0078	0.4%

(c) Differentiated allocation #2

Fig. 10. Fairness of throughput allocation for *hotspot* traffic pattern. The tables show the maximum, minimum, average, and standard deviation of throughputs for each group of flows.

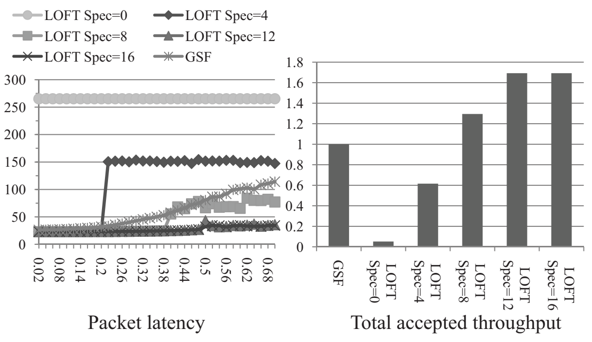

(a) Uniform Traffic

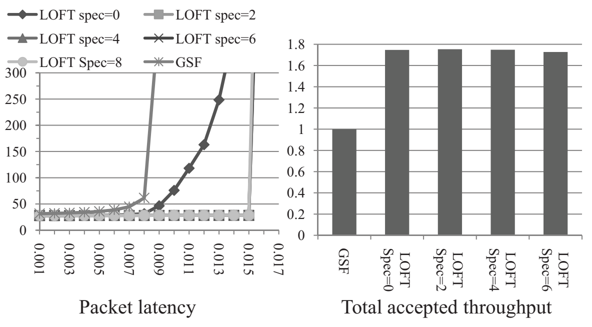

(b) Hotspot Traffic

Fig. 11. Packet latency and network throughput for (a) *uniform* and (b) *hotspot* traffic patterns. Note that throughput results are normalized to that of GSF. For each LOFT architecture, *spec*=N means the speculative buffer size is N.

Figure 11b shows the results for *hotspot* traffic pattern. The performance of LOFT is even better than GSF in this case, where network contention is more fierce. The performance of LOFT is better for all speculative buffer sizes. However, different from the *uniform* case we notice that the speculative buffer size does not significantly impact the performance. This is due to the fact that with high contention on the links speculative switching is least effective.

According to the result above, we choose a 12-flit speculative buffer size, and use this size for the rest of experiment.

6.3. Case Studies of Performance Isolation

We study two cases to exam the effectiveness in performance isolation of LOFT compared with GSF.

a) Case Study I is adapted from the *hotspot* traffic to model the denial-of-service attack. In this case, only nodes 0, 48, and 56 actively send packets to the hotspot, node 63. Each flow is allocated 1/4 of the link bandwidth, that is, 0.25 flits/cycle. $flow_{0\rightarrow 63}$ is a regulated flow, injecting at a constant average rate of 0.2 flits/cycle. $flow_{48\rightarrow 63}$ and $flow_{56\rightarrow 63}$ are aggressors. The injection rates of them varies significantly, and may be well beyond the allocated rate. We assume that both aggressors are injecting at same rates, and measure the performance of each flow versus the injection rate of aggressors.

The results for GSF is shown in Figure 12a. We notice that with the injection rate of aggressors increasing, the average packet latency of all three flows rises significantly. The latency for the regulated flow increases from 60 cycles up to 2000 cycles, which shows that the performance of the regulated flow is severely degraded by the aggressors. In addition, the aggressors also cause the accepted throughput of the regulated flow to slightly decline. Finally, we see that the aggregate throughput is always below 60% of link bandwidth, due to the inefficiency of the flow-control mechanism.

Compared to GSF, the robustness of LOFT is more satisfying as shown in Figure 12b. The packet latencies of all flows do not significantly increase until the aggressor injection rate reaches 0.4 flits/cycle. Beyond that point, all flows see a packet latency increase. However, the latency increase (from 42 cycles to 55 cycles) of the regulated flow is to a much less extent than the aggressors (from $\sim$25 cycles to $\geq$400 cycles). Therefore LOFT provides better performance isolation than GSF, and tends to penalize aggressors that try to exhaust bandwidth. In addition, the network utilization of LOFT (over 90%) is much higher than GSF.

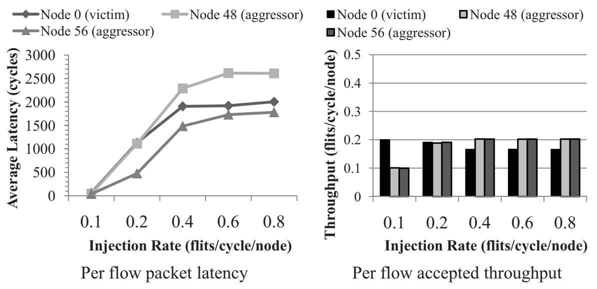

(a) GSF

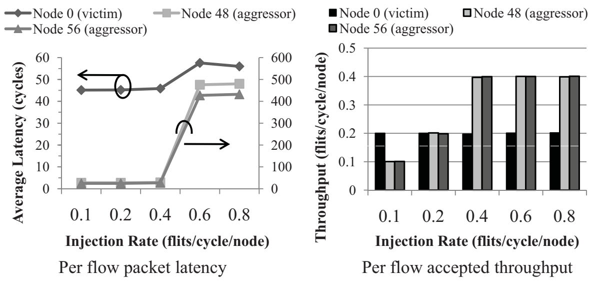

(b) LOFT

Fig. 12. Case Study I: per flow average packet latency and accepted throughput are plotted against aggressor injection rates, when (a) GSF and (b) LOFT are used.

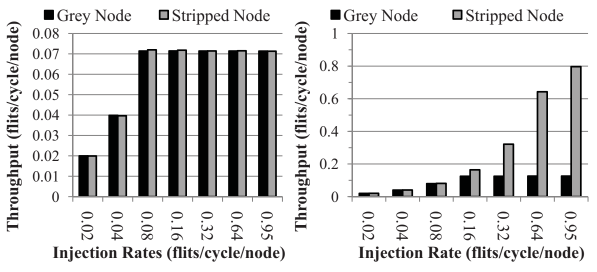

(a) GSF (b) LOFT

Fig. 13. Case Study II: accepted throughputs of grey and stripped nodes in Figure 1 for (a) GSF and (b) LOFT. It is assumed that both kinds of nodes are injecting at the same rates.

b) Case Study II uses the pathological example we previously show in Figure 1. We allocate equal reservations to all flows assuming no prior knowledge of the actual traffic pattern. Furthermore we assume all flows are injecting at same rates, and measure the accepted throughput versus the injection rate. Figure 13 shows the results for both (a) GSF and (b) LOFT. It can be seen that in GSF the stripped node is throttled with the grey nodes due to contention around the hotspot region. In contrast, in LOFT while the throughput of grey nodes saturates early, the stripped node is able to exploit the ample bandwidth exposed to it. LOFT clearly isolates the lightly loaded region from the heavily loaded region in an asymmetrically loaded network. Therefore the overall network utilization and throughput of LOFT is significantly higher than GSF.

7. Conclusion

Providing quality-of-service in network-on-chip is challenging due to the distributed scheduling nature. In this paper we present LOFT, a high performance network-on-chip that provides guaranteed service and overcomes the weaknesses of previous approaches. LOFT combines *locally-synchronized frames*, where each output port independently implements frame-based scheduling, and *flit-reservation*, a pre-scheduling mechanism for efficient flow-control. We compare LOFT with *globally-synchronized frames*, another state-of-the-art QoS framework for NoC. The experiment results show that LOFT achieves equally satisfying fairness, better robustness against denial-of-service attack, and higher network utilization than GSF. We believe LOFT serves as a promising candidate for guaranteed service NoC architectures.

Appendix
Discussion of Condition (1)

In this section, we first formally prove the following theorem.

THEOREM I. With the constraint of condition (1), if the input buffer size is F flits, then at any moment of time and any output port, out_table(i).virtual_credit ≥ 0, $\forall i \in [0, WT-1]$.

Before proving Theorem I, we introduce some necessary mathematical tools:

Preliminaries—First, for the moment we assume infinite frame window and time window. This transformation does not affect the soundness of proof, since we can view the infinite frame/time window as the concatenation of infinite fixed-size frame/time windows. It only removes the ambiguity introduced by wrap-arounds and allows us to conveniently and uniquely identify a frame/time slot. Also for convenience, we use *time slot* (X, a) $(a \in [0, F-1])$ to refer to the $(a+1)$th time slot in frame X.

Furthermore we define

$$\begin{aligned} b(X,a) &= \text{number of data flits scheduled in slot } (X,a) \\ B(X) &= \textstyle\sum_{a=0}^{F-1} b(X,a) \end{aligned}$$

Note that for all valid X and a, $b(X, a)$ is either 0 or 1, and $B(X) \geq 0$. We further define

$$\begin{aligned} u(X,a) &= \text{number of returned virtual credit at slot } (X,a) \\ U(X) &= \textstyle\sum_{a=0}^{F-1} u(X,a) \end{aligned}$$

and for all valid X and a, $u(X, a), U(X) \geq 0$. Given the above notations and supposing the input buffer size is F flits, the virtual credit count of some time slot (X, a) can be calculated as:

$$\begin{aligned} \text{out\_table}(X,a).\text{virtual\_credit} = F - \textstyle\sum_{i=0}^{X-1} B(i) - \sum_{j=0}^{a} b(X,j) \\ + \textstyle\sum_{i=0}^{X-1} U(i) + \sum_{j=0}^{a} u(X,j) \end{aligned} \quad (3)$$

Using equation (3), condition (1) can be transformed into the following equivalent form

$$skipped(IF_{ij}) \geq \sum_{i=0}^{IF_{ij}-1} B(i) - \sum_{i=0}^{IF_{ij}-1} U(i) \quad (4)$$

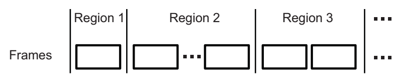

Fig. 14. Divide frame window into frame regions.

Frame Region— We define frame regions as non-overlapping groups of adjacent frames. Figure 14 shows an example of three frame regions. By our convention, a frame region has to contain at least one frame. In addition, we number the frame regions with the frame numbers of the first frames they contain.

Furthermore, we introduce following notations:

$$FR(k) = \text{Frame Region k} \qquad R^{FR}(k)=\sum_{IF_{ij}\in FR(k)} R_{ij}$$
$$B^{FR}(k)=\sum_{X\in FR(k)} B(X) \qquad U^{FR}(k)=\sum_{X\in FR(k)} U(X)$$

Due to space limits, we state the following lemma without a formal proof.

LEMMA I. With the constraint of condition (1), if the input buffer size is F flits, then for frame region $FR(0)$ containing the first frame (frame 0), $R^{FR}(0) \geq B^{FR}(0) - U^{FR}(0)$.

Now we are ready to prove Theorem I with the help of Lemma I.

Proof of Theorem I—Take an arbitrary entry (X, a) in the output scheduling table. We construct a frame region $FR(0)$ containing frame 0 to frame $(X-1)$, and a frame region $FR(X)$ containing only frame X. From Lemma I, we know that $R^{FR}(0) \geq B^{FR}(0) - U^{FR}(0)$. In addition, it is straightforward to see that $\sum_{j=0}^{a} b(X,j) \leq B(X) \leq R^{FR}(X) + R^{FR}(0) - skipped(X)$. Recall that with condition (4), we have $skipped(X) \geq B^{FR}(0) - U^{FR}(0)$. In summary, the virtual credit count of slot (X,a) can be calculated as follows.

$$\begin{aligned}\text{out\_table}(X,a).\text{virtual\_credit} &= F - B^{FR}(0) + U^{FR}(0)\\ &\quad - \textstyle\sum_{j=0}^{a} b(X,j) + \sum_{j=0}^{a} u(X,j)\\ &\geq F - R^{FR}(0) - R^{FR}(X)\end{aligned}$$

Since by construction $R^{FR}(0) + R^{FR}(X) \leq \sum R_{ij} \leq F$, out_table$(X,a)$.virtual_credit ≥ 0 is true for any valid X and a and Theorem I is proven. ■

In addition, condition (4) implies that aggressive flows cannot inject into a frame if the virtual credits consumed in previous frames have not been returned; instead, the aggressive flow $flow_{ij}$ will advance its injection frame pointer and thus $skipped(IF_{ij})$ is increased by C_{ij}. Effectively, **aggressive flows voluntarily yield buffer space to moderate flows when condition (1)/(4) is not satisfied**.

References

[1] Intel Core^{TM} i7 Processor Families. Intel Corporation. [Online]. Available: http://www.intel.com/design/corei7/

[2] L. Seiler, D. Carmean, E. Sprangle *et al.*, "Larrabee: a many-core x86 architecture for visual computing," *ACM Trans. Graphics*, vol. 27, no. 3, pp. 1–15, 2008.

[3] Tilera Processor Families. Tilera Corporation. [Online]. Available: http://www.tilera.com/products/processors.php

[4] T. G. Mattson, R. Van der Wijngaart, and M. Frumkin, "Programming the Intel 80-core network-on-a-chip terascale processor," in *Proc. of Conference on Supercomputing*, 2008, pp. 1–11.

[5] J. Howard, S. Dighe, Y. Hoskote *et al.*, "A 48-core IA-32 message-passing processor with DVFS in 45nm CMOS," in *Digest of Technical Papers in Solid-State Circuits Conference*, 7-11 2010, pp. 108 –109.

[6] R. Iyer, "CQoS: a framework for enabling QoS in shared caches of CMP platforms," in *Proc. of International Conference on Supercomputing*, 2004, pp. 257–266.

[7] K. J. Nesbit, J. Laudon, and J. E. Smith, "Virtual private caches," in *Proc. of International Symposium on Computer architecture*, 2007, pp. 57–68.

[8] S. Srikantaiah, R. Das, A. K. Mishra *et al.*, "A case for integrated processor-cache partitioning in chip multiprocessors," in *Proc. of the Conference on High Performance Computing Networking, Storage and Analysis*, 2009, pp. 1–12.

[9] K. J. Nesbit, N. Aggarwal, J. Laudon *et al.*, "Fair queuing memory systems," in *Proc. of International Symposium on Microarchitecture*, 2006, pp. 208–222.

[10] O. Mutlu and T. Moscibroda, "Stall-time fair memory access scheduling for chip-multiprocessors," in *Proc. of International Symposium on Microarchitecture*, 2007, pp. 146–160.

[11] E. Ebrahimi, C. J. Lee, O. Mutlu *et al.*, "Fairness via source throttling: a configurable and high-performance fairness substrate for multi-core memory systems," in *Proc. of Architectural Support for Programming Languages and Operating Systems*, 2010, pp. 335–346.

[12] J. W. Lee, M. C. Ng, and K. Asanovic, "Globally-synchronized frames for guaranteed quality-of-service in on-chip networks," in *Proc. of International Symposium on Computer Architecture*, 2008, pp. 89–100.

[13] B. Grot, S. W. Keckler, and O. Mutlu, "Preemptive virtual clock: a flexible, efficient, and cost-effective QoS scheme for networks-on-chip," in *Proc. of International Symposium on Microarchitecture*, 2009, pp. 268–279.

[14] K. Goossens, J. Dielissen, and A. Radulescu, "Æthereal network on chip: concepts, architectures, and implementations," *IEEE Trans. Design and Test*, vol. 22, no. 5, pp. 414–421, 2005.

[15] M. Millberg, E. Nilsson, R. Thid, and A. Jantsch, "Guaranteed bandwidth using looped containers in temporally disjoint networks within the Nostrum network on chip," in *Proc. of Conference on Design, Automation and Test in Europe*, 2004, pp. 890–895.

[16] T. Bjerregaard and J. Sparso, "A router architecture for connection-oriented service guarantees in the MANGO clockless network-on-chip," in *Proc. of Conference on Design, Automation and Test in Europe*, 2005, pp. 1226–1231.

[17] W.-D. Weber, J. Chou, I. Swarbrick, and D. Wingard, "A quality-of-service mechanism for interconnection networks in system-on-chips," in *Proc. of Conference on Design, Automation and Test in Europe*, 2005, pp. 1232–1237.

[18] J. H. Kim and A. A. Chien, "Rotating combined queueing (RCQ): bandwidth and latency guarantees in low-cost, high-performance networks," in *Proc. International Symposium on Computer architecture*, 1996, pp. 226–236.

[19] R. Das, O. Mutlu, T. Moscibroda, and C. R. Das, "Application-aware prioritization mechanisms for on-chip networks," in *Proc. of International Symposium on Microarchitecture*, 2009, pp. 280–291.

[20] L.-S. Peh and W. J. Dally, "Flit-reservation flow control," *IEEE Trans. on Parallel and Distributed Systems*, vol. 3, no. 3, pp. 194–205, 2000.

[21] H. Zhang and S. Keshav, "Comparison of rate-based service disciplines," in *Proc. of Conference on Communications architecture & protocols*, 1991, pp. 113–121.

[22] J. Kim, D. Park, C. Nicopoulos, N. Vijaykrishnan, and C. R. Das, "Design and analysis of an NoC architecture from performance, reliability and energy perspective," in *Proc. of ACM symposium on Architecture for Networking and Communications Systems*, 2005, pp. 173–182.

[23] L.-S. Peh and W. J. Dally, "A delay model and speculative architecture for pipelined routers," in *Proc. of International Symposium on High-Performance Computer Architecture*, 2001, p. 255.

[24] S. Li, J. H. Ahn, R. D. Strong, J. B. Brockman, D. M. Tullsen, and N. P. Jouppi, "McPAT: An Integrated Power, Area, and Timing Modeling Framework for Multicore and Manycore Architectures," in *Proc. of International Symposium on Microarchitecture*, 2009, pp. 469–480.

[25] D. Vantrease, N. Binkert, R. Schreiber, and M. H. Lipasti, "Light speed arbitration and flow control for nanophotonic interconnects," in *Proc. of International Symposium on Microarchitecture*, 2009, pp. 304–315.